

ORIGINAL ARTICLE

Mean Electric Field of Dielectric Nanoparticle

Levan Chkhartishvili *, Shorena Dekanosidze, Ramaz Esiava

Chkhartishvili L, Dekanosidze S, Esiava R. Mean Electric Field of Dielectric Nanoparticle. *Int J Adv Nano Comput Anal.* 2023;2(2):62-75.

Abstract

The nanoscale effect of the formation of an electric field near the surface of a dielectric nanoparticle is discussed within the framework of the proposed model based on the reconstruction of the crystal surface, including the splitting of the surface atomic

layer into two parallel sublayers consisting of atoms with only positive or only negative effective static electric charges, respectively. The mean electric field potential and strength are obtained depending on the distance from the surface and the numerical values of their parameters for hexagonal boron nitride are estimated.

Key Words: *Nanoparticle; Crystal surface reconstruction; Static atomic charge; Electric field*

Introduction

A new nanoscale effect of formation an electric field near the surface of dielectric nanoparticles was proposed in [1]. It is based on the surface reconstruction that occurs in some crystals, which involves the splitting of the surface atomic layer into two parallel sublayers consisting of atoms with only positive or only negative effective electrical charges, respectively. The fact is that in a

macroscopic crystal with an almost infinite surface, the electric field of such a surface electric dipole is almost completely concentrated between the sublayers, while in a nanocrystallite of a sufficiently small sizes, an electric field of certain magnitude is also induced outside the sublayers. This can significantly increase the physical reactivity of nanoparticles [2].

Department of Engineering Physics, Georgian Technical University, 77 Merab Kostava Avenue, Tbilisi 0160, Georgia

**Corresponding author: Levan Chkhartishvili, Department of Engineering Physics, Georgian Technical University, 77 Merab Kostava Avenue, Tbilisi 0160, Georgia, Tel: +995 599 34 07 36; E-mail: levanchkhartishvili@gtu.ge*

Received: October 22, 2023, Accepted: December 22, 2023, Published: December 27, 2023



This open-access article is distributed under the terms of the Creative Commons Attribution Non-Commercial License (CC BY-NC) (<http://creativecommons.org/licenses/by-nc/4.0/>), which permits reuse, distribution and reproduction of the article, provided that the original work is properly cited and the reuse is restricted to noncommercial purposes.

Because of physical reactivity and related adsorption selectivity for different molecules from gaseous and liquid media, nanopowders with sufficiently large specific surface area are considered as useful materials for environmental protection, e.g., as hydrogen-fuel nanoreservoirs for “green energetics” or in water treatment for removal of organic pollutants. Effective removal of oils, organic solvents and dyes from water is very important for protection of the environment and water sources.

For example, so-called activated h-BN was reported as an effective adsorbent for pollutants in water and air as well. It exhibits a superhigh surface area, a large pores volume and a multimodal microporous/mesoporous structure. Listed properties yield in its excellent adsorption performance for some heavy metal ions and organic pollutants (such as tetracycline, methyl orange, Congo red, etc.) in water, as well as volatile organic compounds (e.g., benzene) in air. The high reusability has also been confirmed for activated boron nitride. As adsorbed it can be easily regenerated by a simple thermal treatment in air: almost all the adsorbates are removed without losses of the BN.

The theoretical model of layered binary compounds, namely hexagonal boron nitride h-BN, proposed in [3] can explain the selectivity of their surface to the adsorption of various particles from gases or liquids. The weakness of the interaction between layers compared to the intralayer bonding makes it possible to reconstruct the surface layer in such a way that different atoms are displaced in opposite directions from the surface plane. Since the bond in h-BN crystals is partially ionic, i.e. boron B and

nitrogen N atoms have non-zero effective static electric charges of opposite signs, and then during reconstruction the surface becomes polarized and attracts some atomic and molecular ions as well as dipoles of molecules from the medium. The efficiency of their adsorption depends on the relationship between electrostatic / polarization attraction and Pauli repulsion forces between these particles and the crystal surface.

To be able to obtain at least numerical estimates of such kind, together with above model we introduced a very simplified theory of h-BN crystals surface reconstruction. It allowed to estimate the dipole layer thickness based on intra- and interlayer bond lengths and static positive and negative electric charges attributed to B and N atoms, respectively, in h-BN crystals. Then, h-BN surface binding parameters were estimated for a few ions and polar and nonpolar molecules.

According to these calculations, the binding energies to the h-BN surface can be significantly different for different ionic and molecular species. That is why further research in this direction is important from both academic and applied points of view.

Model Construction

The real, that is, the finite crystal is a polyhedron faceted by certain polygonal fragments of atomic layers. For simplicity of consideration, we replace each of these polygons with a circle of certain radius r providing the same area s :

$$s = \pi r^2 \quad (1)$$

In general, after reconstruction any atomic layer of the free surface of an electrically neutral dielectric crystal has some non-zero static electric charge $\pm q$, where $q > 0$ denotes the absolute value of the surface charge. It is natural to assume that the compensating charge $\mp q$ completely belongs to the subsequent atomic layer.

Again, for simplicity and taking into account the purpose of calculating the mean crystal surface electric field, we assume that the static electric charges on crystal surface and subsequent atomic layers, respectively, are distributed continuously and evenly with uniform surface densities $\pm\sigma$ of

$$\pm\sigma = \pm \frac{q}{s} \quad (2)$$

For clarity, let us analyze the situation when surface and subsequent atomic layers are charged positively and negatively, respectively.

Let us choose a cylindrical coordinate system (ρ, θ, z) , the Oz axis of which is normal to the crystal surface, and the system origin O is located at the midpoint between the centers of two circles modeling the charged surface and subsequent atomic layers. The elementary area ds of any such surface (Figure 1) and the associated elementary electric charges $\pm dq$ are expressed as:

$$ds = \rho d\rho d\theta \quad (3)$$

and

$$\pm dq = \pm\sigma ds = \sigma\rho d\rho d\theta \quad (4)$$

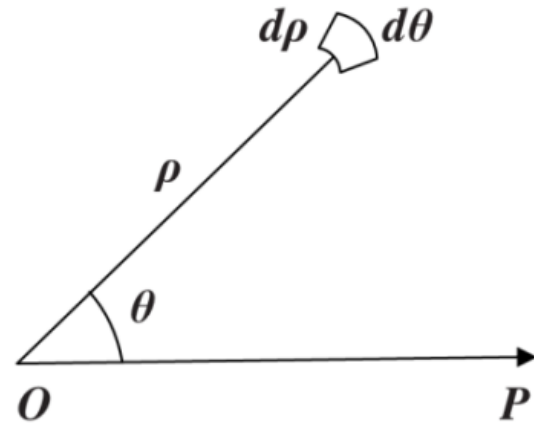


Figure 1) Calculation of plane elementary area in polar coordinates.

Let d be the distance between two parallel surface atomic layers. The corresponding circles are then placed in the $z = \pm d/2$ planes: see Figure 2. In Gaussian units, the potential φ of the crystal surface electric field at the (R, θ, z) current point (Figure 3) is equal to:

$$\begin{aligned} \varphi(R, \theta, z) &= \\ &= \sigma \sum_{\pm} (\pm) \int_0^r d\rho \rho \int_0^{2\pi} \frac{d\theta}{\sqrt{(R \cos \theta - \rho \cos \theta)^2 + (R \sin \theta - \rho \sin \theta)^2 + (z \mp \frac{d}{2})^2}} \\ &= 2\sigma \sum_{\pm} (\pm) \int_0^r d\rho \rho \int_0^{2\pi} \frac{d\theta}{\sqrt{4R^2 + 4z^2 \mp 4dz + d^2 + 4\rho^2 - 8R\rho \cos(\theta - \theta)}} \quad (5) \end{aligned}$$

The mean value of the term $8R\rho \cos(\theta - \theta)$, which is proportional to the cosine of the integration variable θ linear function, is zero whereas the mean values of terms $4R^2$ and $4\rho^2$ are equal positive constants less than r^2 , the surface charges circles' radius square. The concept of mean electric field has physical meaning only at distances z significantly exceeding the size-parameters r and d of its source, the fragment of a crystal surface: $z \gg r$ and $\gg d$. Consequently, mean of the sum $\mp 4dz + d^2 + 4\rho^2 - 8R\rho \cos(\theta - \theta)$ in integrand can be assumed significantly less than that of the

sum $4R^2 + 4z^2$. Then expanding the integrand into a power series of this small parameter and retaining only zeroth- and first-order terms we get approximately:

$$\begin{aligned} \varphi(R, \theta, z) &\approx \frac{\sigma}{\sqrt{R^2+z^2}} \sum_{\pm} (\pm) \int_0^r d\rho \rho \int_0^{2\pi} d\theta \left(1 - \frac{\mp 4dz + d^2 + 4\rho^2 - 8R\rho \cos(\theta - \theta)}{8(R^2+z^2)} \right) \\ &= \frac{2\pi\sigma}{\sqrt{R^2+z^2}} \sum_{\pm} (\pm) \int_0^r d\rho \rho \left(1 - \frac{\mp 4dz + d^2 + 4\rho^2}{8(R^2+z^2)} \right) \\ &= \frac{2\pi\sigma dz}{(R^2+z^2)\sqrt{R^2+z^2}} \int_0^r d\rho \rho \\ &= \frac{\pi\sigma r^2 dz}{(R^2+z^2)\sqrt{R^2+z^2}} \equiv \varphi(R, z) \end{aligned} \tag{6}$$

Thus, there is in fact no angular dependence, $(R, \theta, z) \rightarrow \varphi(R, z)$, as expected from the model symmetry.

Consider in the coordinate system (R, θ, z) a circle of radius r lying in the plane $z = 0$, the center of which coincides with its origin. The area S of this circle is equal to that of the parallel crystal facet:

$$S = s = \pi r^2 \tag{7}$$

The corresponding elementary area, i.e., the increase in the area of a circle of radius R , when it increases by dR (Figure 4), is:

$$dS = d(\pi R^2) = 2\pi R dR \tag{8}$$

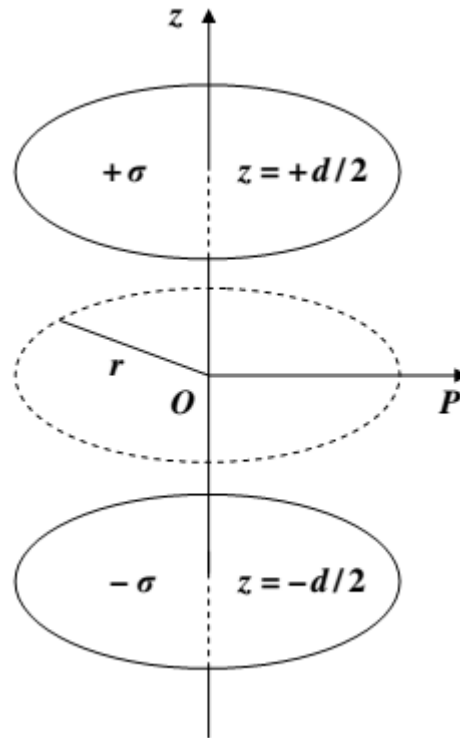


Figure 2) Geometric model of reconstructed crystal surface.

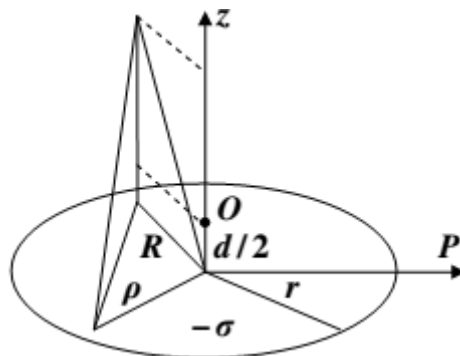


Figure 3) Example of calculating of distance between elementary area of charged surface and current point in space.

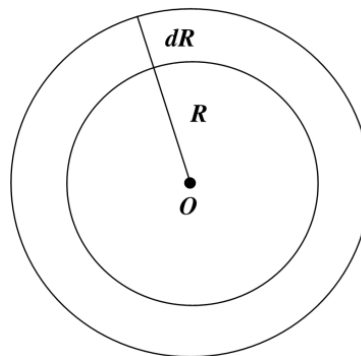


Figure 4) Calculating of elementary area of circle and current point in space.

Then the mean value $\varphi(z)$ of the crystal electric field potential over its surface area S can be found as:

$$\begin{aligned}\varphi(z) &= \frac{1}{\pi r^2} \int_0^r d(\pi R^2) \varphi(R, z) \\ &= \frac{2}{r^2} \int_0^r dR R \varphi(R, z) \\ &= 2\pi\sigma dz \int_0^r \frac{dR R}{(R^2+z^2)\sqrt{R^2+z^2}} \\ &= 2\pi\sigma d \left(1 - \frac{z}{\sqrt{r^2+z^2}}\right)\end{aligned}\quad (9)$$

Introducing the potential value at the crystal surface

$$\varphi_0 = \varphi(0) = 2\pi\sigma d \quad (10)$$

we have that

$$\frac{\varphi(z)}{\varphi_0} = 1 - \frac{1}{\sqrt{1+\frac{r^2}{z^2}}}\quad (11)$$

Nanocrystal surface electric field strength vector is directed to its normal, i.e., has only z -component $E_z(z) = E(z)$. Introducing the electric field strength magnitude at the crystal surface

$$E_0 = E(0) = \frac{2\pi\sigma d}{r} \quad (12)$$

we finally obtain that,

$$E(z) = \frac{d\varphi(z)}{dz} = \frac{E_0}{\left(1+\frac{z^2}{r^2}\right)\sqrt{1+\frac{z^2}{r^2}}}\quad (13)$$

or

$$\frac{E(z)}{E_0} = \frac{E_z(z)}{E_0} = \frac{1}{\left(1+\frac{z^2}{r^2}\right)\sqrt{1+\frac{z^2}{r^2}}}\quad (14)$$

The formation of an electric field near the surface of a hexagonal boron nitride nanoparticle is determined by two factors: (i) its layered crystal structure, regardless its constituent layers have a hexagonal 2D-crystalline structure or not; and (2) partial ionicity of intralayer B–N bonds. As for the disk-like morphology of h-BN nanoparticles, which roughly resembles a hexagonal shape, it is not associated with the presence of hexagonal atomic layers in this crystal, but again with its layered 3D-crystalline structure. Therefore, other inorganic particles with a hexagonal shape (zinc oxides, gold, silver, iron, etc.) but without a layered crystalline structure are not expected to produce any detectable surface field.

As for graphene in the form of graphite few-layer fragment, it certainly has a layered crystalline structure (similar to h-BN, but with rotated atomic layers), but is an elementary phase of carbon C. The adsorption activity demonstrated by few-layer graphene should be attributed to the polarization of its surface due to the electron charge displacement from low-coordinated surface atoms to highly coordinated ones in the bulk.

Results and Discussion

Taking into account the relationship between the surface densities of the electric charge and the electric dipole moment in the crystal surface and subsequent atomic sublayers charged positively or negatively, we state that the expressions obtained here for the mean electric field potential and strength of a nanoparticle agrees well with that obtained earlier in [1] for a disk-like nanoparticle on its axis.

We see that both the potential and the electric field strength have finite values on the surface ($z = 0$)

$$\varphi(0) = \varphi_0 \quad (15)$$

and

$$E(0) = E_0 \quad (16)$$

and tend to zero at infinity ($z \rightarrow \infty$):

$$\varphi(z \rightarrow \infty) \rightarrow \frac{\varphi_0 r^2}{2z^2} \rightarrow \frac{1}{z^2} \rightarrow 0 \quad (17)$$

and

$$E(z \rightarrow \infty) \rightarrow \frac{E_0 r^3}{z^3} \rightarrow \frac{1}{z^3} \rightarrow 0 \quad (18)$$

Constructed model contains two parameters: surface density of static electrical charges σ and surface dipole layer thickness. Let us find their numerical estimates for h-BN crystal surface.

In ab initio calculations performed [4] on small $B_{12}N_{12}$ clusters, a buckling of the BN bond was observed for a monocyclic ring structure. Total energy minimization based on the DFT (Density Functional Theory) within the LDA (Local Density Approximation) have been performed which indicated a buckling of the B–N bond [5]. The main relaxation effect is a buckling of the B–N bond, together with a small ($\sim 1\%$) contraction of the bond length. Due to electron charge transfer from boron to nitrogen, the buckled tubular structure forms a dipolar shell. The distance between the inner B-cylinder and the outer N-cylinder is, at constant radius, mostly independent of tube helicity and decreases from 0.2 a.u.

≈ 0.10 Å for the (4,4) tube to 0.1 a.u. ≈ 0.05 Å for the (8,8) tube. By the MD (Molecular Dynamics) simulations, it was also shown [6] that relaxation of a nanotubular structure leads to the formation of a wavy surface, on which B and N atoms rotate inward and outward, respectively, reminiscent of the surface relaxation of bulk III–V compounds.

Electrostatic potentials on both the outer and inner surfaces of single-walled BN nanotube model systems were calculated [7] using a HF (Hartree-Fock) level of theory approach. The BN tubes were found to have strong and variable surface potentials, and their internal surfaces were noticeably positive. Thus, the reconstruction of the surface of boron nitrides with both flat and tubular layered structures consists of splitting the surface atomic layer into two – upper and lower – sublayers of atoms with negative and positive effective charges, respectively. The opposite charges of these surface sublayers are associated with the opposite static charges of the B (positive) and N (negative) atoms in this compound.

As mentioned above, in a layered crystal the most likely reconstruction of its surface is the displacement of various atoms in opposite directions from the layer. Indeed, it has been demonstrated by MD study [8] that the lowest energy surface defect in a single hexagonal BN layer involves out-of-plane displacement of the N atom to form a tetrahedron with three in-plane B atoms. Obviously, the displacements of all N atoms are equivalent to the displacements of all B atoms in the opposite direction. The same applies to BN nanotubes, the BN hexagonal layers wrapped into cylinders.

Using ab initio simulations of electron dynamics under IR (InfraRed) laser illumination, it was found [9] that exposing h-BN to a laser of a certain wavelength causes lattice vibrations with B and N atoms moving in opposite directions. Since these atoms have effective electric charges of opposite signs, such vibrations give rise to dynamic dipoles. The possibility of forming a dynamic dipole layer from a single hexagonal layer in BN crystal serves as an additional argument in favor of the possibility of forming a static dipole layer from a free surface layer as a result of its reconstruction. Excited state MD calculations using time-dependent DFT show a transient interlayer contraction of h-BN due to an interlayer dipole–dipole attraction. The interlayer distance of the bilayer h-BN sheet was initially set as 3.274 Å. For the optical frequency resonant with the A_{2u} lattice vibration, the contraction was large: up to 0.37 Å (11.3% of the original interlayer distance).

Assuming that surface reconstruction compensates for the binding energy imbalance resulting from the destruction of interlayer bonds, the thickness of the surface dipole layer in h-BN was estimated as 0.14 Å [3]. In this work, this and above theoretical predictions on the reconstruction of ideally flat/cylindrical BN surfaces with hexagonal atomic structure are indirectly supported by experimental finding of intensive radial vibrations visible in the Raman spectra of BN nanotubes.

The mechanism of direct (without the participation of catalyst substances) polymorphic transformation of hexagonal boron nitride h-BN into sphalerite, i.e., cubic

boron nitride c-BN can be represented [10] as follows (the same is true for the transformation of rhombohedral boron nitride r-BN into wurtzite boron nitride w-BN). Under certain external influences, neighboring B and N atoms in different hexagonal layers are displaced towards each other, forming a strong (partially ionic) covalent bond instead of a weak (partially ionic) van der Waals bond (Figure 5). With this transformation, the projection length of B–N covalent bonds changes insignificantly: $b_{h-BN p} = b_{h-BN} = 1.4457$ and $b_{c-BN p} = 1.4774$ Å, while the length of interlayer van der Waals bonds in h-BN decreases significantly when converted to a covalent bond in c-BN: $b'_{h-BN} = 3.3305$ and $b_{c-BN} = 1.5670$ Å.

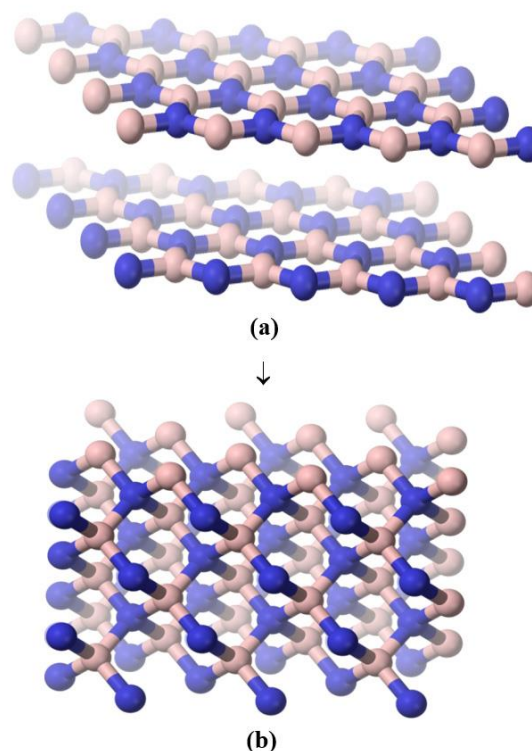


Figure 5) crystalline structures of (a) hexagonal and (b) cubic boron nitrides.

We image the free surface reconstruction in h-BN based on $h-BN \rightarrow c-BN$ structural

transformation mechanism taking into account two additional factors:

- The atomic radius of nitrogen N exceeds that of boron B. In the h-BN structure, the electron cloud is shifted from boron atoms towards nitrogen atoms and moreover, the ionic radius of negative nitrogen ions exceeds that of positive boron ions.
- The equivalence of all B–N bonds in the c-BN crystal leads to the conclusion that the corresponding bond length represents the equilibrium distance between neighboring B and N atoms. In the hexagonal layer, the shorter bond length is fixed due to the presence of neighboring layers on both sides in the h-BN crystal.

Thus, surface reconstruction in h-BN would look like the displacement of N atoms beyond the surface to a distance corresponding to the equilibrium bond length in c-BN (Figure 6). From this model, dipole layer thickness can be calculated as:

$$d = \sqrt{b_{c-BN}^2 - b_{h-BN}^2} \approx 0.6045 \text{ \AA} \quad (19)$$

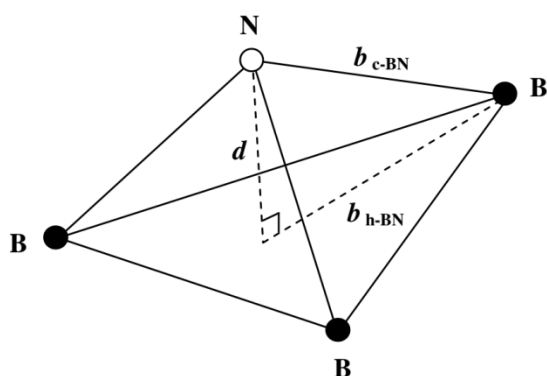


Figure 6) Fragment of hexagonal boron nitride reconstructed surface.

Static atomic charges, although they affect all the physical properties of a material

through its electronic structure, are difficult to measure parameters: the corresponding dependences are too complex and do not allow determining their values. To respond this challenge, a method was developed [11,12] for semiempirical estimation of atomic charges in binary compounds based on empirical parameters (number of atomic pairs in a unit cell, lattice constants, Young's modulus and dielectric constant). In particular, in the intralayers of h-BN the effective atomic charge number N is found to be around 0.35. Area of 2D unit cell of h-BN containing 1 boron and 1 nitrogen atoms is,

$$s_{h-BN} = \frac{3\sqrt{3}b_{h-BN}^2}{2} \quad (20)$$

Then surface density of static electrical charge for h-BN crystal is determined as:

$$\sigma = \frac{Ne}{s_{h-BN}} = \frac{2Ne}{3\sqrt{3}b_{h-BN}^2} \approx 0.064 \text{ e/\AA}^2 \quad (21)$$

where e is the elementary electric charge. The total surface dipole on the h-BN nanosheet can be indicated with elemental dipole arrows (Figure 7).

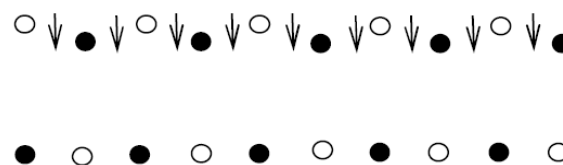


Figure 7) Side view of surface dipole on hexagonal boron nitride nanosheets indicated with elemental dipoles (\bullet – boron and \circ – nitrogen).

Note that for layered crystals and, in particular, h-BN, based on both experimental and theoretical arguments, a disk-shaped morphological model was introduced [13-15], which corresponds well to the

approximation used above, replacing crystal polygonal face with a circle.

To the best of our knowledge, there are no experimental values available for electrostatic forces/charges on the nanoparticles surface. The proposed model contains two parameters: surface dipole layer thickness and static electric charge surface density. For the h-BN crystal, we have determined both of them: as 0.6045 \AA and 0.064 e/\AA^2 , respectively. Based on these values, it is possible to calculate surface electric field potential and strength for a given average radius of h-BN nanopowder disk-like particles.

Finally, let briefly overview the problems reported in the literature those need consideration taking into account nanoparticles electric field.

An eigenoscillation method version was applied [16] for describing the radiation properties of nanoparticles. Their electromagnetic field was presented in terms of Debay potentials. Introducing the corresponding boundary conditions determines the eigenvalues and eigenfunctions of respective homogeneous problem and, in turn, the electromagnetic field components. The numerical results testify the effectiveness of the approach used.

Co-doped SiC powders with core/shell heterogeneous nanoarchitectures were synthesized [17] through mechanically activation-assisted combustion. Co-doping enhances the SiC high-temperature dielectric

and microwave absorption properties. The Co dopants introduce abundant defects in SiC, such as V_C , Co_{Si} and $Co_{Si}V_C$, which can work as dipoles to promote the polarization loss, and create more carriers to increase the according leakage loss. In addition, these core/shell nanoarchitectures can result in interfacial polarization between the shell surface and the core to further enhance the dielectric loss and consequently improve the microwave absorption performance. Thus, combining doping and fabricating core/shell nanoarchitecture would be an effective route for designing high-temperature microwave inorganic absorbers.

The junction between the organic semiconductor and insulator increases the conductivity of conjugated material. To explain this phenomenon, a lamellar system based on R-P3HT–regioregular poly (3-hexylthiophene and P4VP–poly (4-vinylpyridine) cross-linked with d-block metal complexes was studied [18]. Bilayer samples, mimicking organic FET (Field Effect Transistor) were fabricated by R-P3HT thin film casting, subsequent P4VP film casting on its top, and cross-linking of the P4VP surface. The Co- and Zn-complexes exist only on the bilayer surface and do not penetrate the semiconductor. The conductivity of the system increases with each preparation step, to reach a value four orders higher as compared to the as-cast R-P3HT. The described effect is shown to be a consequence of the contact of R-P3HT and P4VP, namely, attributed to the electric field induced in the semiconductor area by the

pyridine dipole moments directed by surface-oriented metal complex.

According to the study [19] of optical textures and director configurations within nematic-in-water microdroplets of the liquid-crystalline mixtures based on azoxybenzene and cyanobiphenyl as a polar dopant, both of them as pure materials exhibit bipolar configuration within liquid-crystalline droplets, whereas their mixtures at appropriate concentrations spontaneously form radial droplets. Increasing of the dopant's concentration resulted in the forward tangential-homeotropic and reentrant homeotropic-tangential anchoring transitions. Bipolar-to-radial structural transition could be also triggered by UV (UltraViolet) irradiation providing nematogens isomerization. Critical irradiation time for radial configuration formation decreases with concentration of polar dopant.

Green synthesis of zinc oxide ZnO nanoparticles was studied [20] using a novel natural source and zinc nitrate $Zn(NO_3)_2$ as Zn^{2+} source. Parameters such as concentration, time, temperature and pH have a direct impact on the synthesis process. Synthesized nanoparticles are mainly spherical or oval with an average size of about 7 nm. The effect of antimicrobial nanoparticles calculated using disk diffusion method.

Zinc oxide nanoparticles produced using natural resources show [21] significant antibacterial activity. Then they can be used

as a new generation of antimicrobial agents, for example, toothpaste containing zinc nanoparticles can be prescribed for patients with immune deficiency to prevent the growth of microbial pathogens in the mouth and its transmission to the body.

Study [22] examined the potential of ZnO-NPs (Zinc Oxide NanoParticles) fabricated using the *Caryophyllus aromaticus* leaf extract to inhibit MDR (MultiDrug-Resistant) *Acinetobacter baumannii* infection. Analytical results confirmed the stable ZnO-NPs fabrication with crystalline nature and mean particle size of 18 nm. ZnO-NPs were considered as potent anti-MDR agent for efficient therapy.

The work [23] showed the synthesis of ZnO-NPs using leaf extract of *Punica granatum*. Characterization showed the synthesis of stable crystalline ZnO-NPs with an average size of 7 nm. The results revealed the dose dependent cytotoxicity, indicating their prospects for the development of novel techniques and materials for pediatric leukemia cancer therapy.

Conclusions

To highlight the possible applications of the obtained results, we first briefly summarize the available information on the surface properties of hexagonal boron nitride those are of practical interest.

As early as 1992, the adsorption of organic molecules on the h-BN surface was studied [24], aiming at the analysis of oil refinery products. It was found that if the number of

contacts of adsorbent molecules with flat areas of the basic faces of the h-BN crystal is considered for the main factor determining the surface homogeneity, the samples with the most homogeneous surface revealed the minimal adsorption and vice versa – the samples with a sufficiently high specific surface revealed the existence of a significant number of active adsorption centers. Note, the h-BN surface becoming more homogeneous after its modification by the adsorption of organic molecules reveals that already adsorbed molecules additionally capture adsorbent layers from the environment.

So-called activated BN was reported in [25] as an effective adsorbent for pollutants in water and air. The obtained material exhibited a super high surface area ($2078 \text{ m}^2/\text{g}$), a large pore volume ($1.66 \text{ cm}^3/\text{g}$) and a multimodal microporous/mesoporous structure (located at distances of about 1.3, 2.7 and 3.9 nm). Activated BN also exhibited an excellent adsorption performance for various metal ions (Cr^{3+} , Co^{2+} , Ni^{2+} , Ce^{3+} and Pb^{2+}) and organic pollutants (tetracycline, methyl orange and Congo red) in water, as well as volatile organic compounds (benzene) in air. Its high reusability also was confirmed. As-adsorbed activated BN can be easily regenerated by a simple thermal treatment route at 400°C for 2 h in air: almost all the combustible adsorbate is removed without any loss of the BN. It was stated that a considerable degree of ionicity of B–N bonds makes the BN materials highly preferred for the adsorption of the pollutants.

It was reported [26] that porous boron nitride nanosheets with very high specific surface area exhibit excellent sorption performances for a wide range of oils, solvents and dyes. The nanostructured material adsorbs/absorbs up to 33 times its own weight in organic substances while repelling water. The saturated BN nanosheets can be readily cleaned for reuse by burning or heating in air because of their strong resistance to oxidation. The interlayer distance can increase by 37% through intercalation of the organic molecules in the interlayer space. Ethanol sorption leads to a smaller expansion of 17%, which might be owing to the alcohol hydrophilicity. Consequently, the increase in the intercalation of molecules in the interlayer space also contributes to the increased uptake of the porous BN nanosheets for oils, and organic solvents and then the mechanism of this process can be ascribed to adsorption of molecules on the hydrophobic BN nanosheets surface and/or capillarity effects for filling of the space between the sheets. The holes inside the nanosheets and the space between the BN layers are mostly hydrophobic. Capillarity effects in the hydrophobic sheets can then only take place with hydrophobic liquids, such as oils. Dyes are either at solid state in their pure form or as dilutes in hydrophilic (aqueous) solutions and cannot contribute to swelling of the nanosheets as a consequence of capillarity filling. Dye sorption then only relies on the surface effect. Nevertheless, the dye sorption capacity of the porous BN nanosheets is still higher than those of most common commercial sorbents. Once it is saturated with the pollutant, the sheet can easily be

cleaned by heating it, burning off the pollutant but leaving the sheet undamaged. This easy recyclability further demonstrates the potential of porous boron nitride nanosheets for water purification and treatment.

In the reviews [27,28], carbon nanostructures, in particular, graphene (G) and its structural analogue – hexagonal boron nitride (h-BN) – sheets are mentioned as good adsorbers/absorbers of big organic molecules. A review [29] was given on BN-based nanoreservoirs for hydrogen storage. Surface nanoscale effect explains the enhancement in physical reactivity of not only nanopowdered but also nanoporous materials with decreasing of particles / porous sizes. See, e.g., report [30], where porous boron nitride microfibers are found to be an effective material capturing pollutants from aqueous solutions. In the review [31], boron nitride (BN) was considered among seven modern and most promising semiconductor materials from the point of view their use in creation of new microelectronic products in the next decade.

In summary:

- A model for reconstructing the free surface of dielectric crystals is presented.

This means representing the finite polygonal face of the crystal as a circle of the same area and splitting the surface atomic layer into two sublayers with static electric charges of the same magnitude but opposite signs. Such a dipole layer is considered as a source of a near-surface electric field.

- Within the framework of the proposed model, the potential and strength of the mean near-surface electric field are calculated depending on the distance from the surface in the direction of its normal.
- These expressions contain two model parameters: the distance d between charged surface sublayers and the magnitude σ of the electric charge surface densities in these sublayers. For the surface of hexagonal boron nitride h-BN layered crystal, they are estimated as: $d \approx 0.6045 \text{ \AA}$ and $\sigma \approx 0.064 e/\text{\AA}^2$.
- A significant surface electric field makes nanopowder and nanoporous dielectric materials physically active and, as a result, promising for various practical applications, in particular, for purifying water from organic pollutants.

References

1. Chkhartishvili L. Nanoparticles near-surface electric field. *Nanoscale Res Lett.* 2016;11:1-4.
2. <https://atlasofscience.org/nanostructure-makes-crystalline-compound-physically-reactive/>
3. Chkhartishvili L, Sartinska L, Ramishvili TM. Adsorption selectivity of boron nitride nanostructures designed for environmental protection. In: Hussain ChM, Kharisov B (eds), *Advanced Environmental Analysis: Applications of Nanomaterials*. Royal Society of Chemistry, Cambridge, England. 2017;pp.167-92.
4. Jensen F, Toftlund H. Structure and stability of C₂₄ and B₁₂N₁₂ isomers. *Chem Phys Lett.* 1993;201:89-96.
5. Blase X, Rubio A, Louie SG, et al. Stability and band gap constancy of boron nitride nanotubes. *Europhys Lett.* 1994;28:335.
6. Menon M, Srivastava D. Structure of boron nitride nanotubes: tube closing versus chirality. *Chem Phys Lett.* 1999;307:407-12.
7. Peralta-Inga Z, Lane P, Murray JS, et al. Characterization of surface electrostatic potentials of some (5,5) and (n,1) carbon and boron/nitrogen model nanotubes. *Nano Lett.* 2003;3:21-8.
8. Slotman GJ, Fasolino A. Structure, stability and defects of single layer hexagonal BN in comparison to graphene. *J Condens Matter Phys.* 2012;25:045009.
9. Miyamoto Y, Zhang H, Miyazaki T, et al. Modifying the interlayer interaction in layered materials with an intense IR laser. *Phys Rev Lett.* 2015;114:116102.
10. Petrescu MI, Balint MG. Structure and properties modifications in boron nitride. Part I: direct polymorphic transformations mechanisms. *UPB Sci Bull B.* 2007;69:35-42.
11. Chkhartishvili LS, Dekanosidze SV, Maisuradze NI. Evaluation of atomic charges in polar crystals. In: Wilson M (ed), *Trends in Modern Science. Science and Education*, Sheffield, England. 2014;pp.51-4.
12. Chkhartishvili L, Dekanosidze S, Maisuradze N, et al. Estimation of atomic charges in boron nitrides. *East Eur J Enterp.* 2015;3:50-7.
13. Chkhartishvili L. Morphology model for nano-powdered boron nitride lubricants. 2nd International Conference "Nanotechnology", Tbilisi, Georgia. 2012.
14. Chkhartishvili L. Correlation between surface specific area and particles average size: hexagonal boron nitride nano-powders. *Nano Studies.* 2012;6:65-76.
15. Tsagareishvili OA, Chkhartishvili LS, Gabunia DL, et al. Calculation of specific surface of nanocrystalline powders of hexagonal boron nitride. *Mater Sci Nanostr.* 2015;2/3/4:69-77.
16. M. Andriychuk. Investigation of radiation properties of nanoparticles by generalized eigenoscillation method. 9th International Conference on Advanced Computer Information Technologies (ACIT), Ceske Budejovice, Czech Republic. 2019.
17. Kuang B, Dou Y, Wang Z, et al. Enhanced microwave absorption properties of Co-doped SiC at elevated temperature. *Appl Sur Sci.* 2018;445:383-90.
18. Dabczynski P, Pawlowska AI, Majcher-Fitas AM, et al. Extraordinary conduction increase in model conjugated/insulating polymer system induced by surface located

- electric dipoles. *Appl Mater Today*. 2020;21:100880.
19. Dubtsov AV, Pasechnik SV, Shmeliyova DV, et al. Influence of polar dopant on internal configuration of azoxybenzene nematic-in-water droplets. *Liq Cryst*. 2018;45:388-400.
 20. Zare E, Pourseyedi Sh, Khatami M, et al. Simple biosynthesis of zinc oxide nanoparticles using nature's source, and its *in vitro* bio-activity. *J Mol Struct*. 2017;1146:96-103.
 21. Aflatoonian M, Khatami M, Sharifi I, et al. Evaluation antimicrobial activity of biogenic zinc oxide nanoparticles on two standard gram positive and gram negative strains. *Tehran Univ Med J*. 2017;75:562-9.
 22. Hou Y, Hou Y, Ren Y, et al. *C. aromaticus* leaf extract mediated synthesis of zinc oxide nanoparticles and their antimicrobial activity towards clinically multidrug-resistant bacteria isolated from pneumonia patients in nursing care. *Mater Res Express*. 2020;7:095015.
 23. Liu Z, Chen F, Lu Z. Biofabrication of zinc oxide nanoparticles, characterization and cytotoxicity against pediatric leukemia cell lines. *Green Process Synth*. 2019;9:56-62.
 24. Daydakova IV. Adsorption and Chromatographic Properties of Thin Layers of Long-Chain hydrocarbons to Surface of Carbon Blacks and Boron Nitride. Lomonosov Moscow State University, Moscow, Russia. 1992.
 25. Li J, Xiao X, Xu X, et al. Activated boron nitride as an effective adsorbent for metal ions and organic pollutants. *Sci Rep*. 2013;3:3208.
 26. Lei W, Portehault D, Liu D, et al. Porous boron nitride nanosheets for effective water cleaning. *Nat Commun*. 2013;4:1777.
 27. Kharisov BI, Dias HR, Kharissova OV. Nanotechnology-based remediation of petroleum impurities from water. *J Pet Sci Eng*. 2014;122:705-18.
 28. Gehrke I, Geiser A, Somborn-chulz A. Innovations in nanotechnology for water treatment. *Nanotechnol Sci Appl*. 2015;8:1-17.
 29. Chkhartishvili L. Hydrogen nanoreservoirs made of boron nitride. In: Kharisov BI, Kharissova OV, Dias HVR (eds), *Nanomaterials for Environmental Protection*. Wiley, Hoboken, New Jersey, U.S. 2014;pp.451-67.
 30. Dai P, Xue Y, Wang X, et al. Pollutant capturing SERS substrate: porous boron nitride microfibers with uniform silver nanoparticle decoration. *Nanoscale*. 2015;7:18992-7.
 31. Demidov AA, Rybalka SB. Modern and promising semiconductor materials for microelectronics of the next decade (2020-2030). *Appl Math Phys*. 2021;53:53-72.